

# VALIDATION OF A NOVEL METHOD FOR THE CALCULATION OF NEAR-FIELD SYNCHROTRON RADIATION \*

F.-Y. Li<sup>†</sup>, C.-K. Huang, R. V. Garimella, T. J. T. Kwan, B. E. Carlsten  
Los Alamos National Laboratory, Los Alamos, NM, USA 87545

## Abstract

The phenomenon of synchrotron radiation (SR) from electrons is at the core of modern accelerator based light sources. While SR in the far field has been well characterized, the near-field SR and its impacts on self-consistent electron beam dynamics remain an ongoing topic. Since it is difficult to experimentally characterize the near fields, it is desirable to develop accurate and efficient numerical methods for the design of these light sources. Here, we investigate a novel method, originally proposed by Shintake and which potentially has both high efficiency and accuracy. We focus on the field calculation of this method and show that the original idea has missed the important terms of fields due to electron acceleration and therefore only applies to a linear motion. To correct this limitation we developed a modified algorithm that gives consistent fields with direct calculations using the Liénard-Wiechert equation. Some basic signatures of the near-field SR fields are also drawn for a cyclotron motion by using this modified approach.

## NEAR-FIELD SYNCHROTRON RADIATION AND ITS MODELING

Synchrotron radiation (SR) in the far field has been well characterized and routinely used in synchrotron beamlines worldwide for advanced applications such as x-ray spectroscopy and structural imaging [1]. Meanwhile, the near-field SR and its impacts on self-consistent electron beam dynamics have only received increasing attention in recent years. The continuing quest for coherent x-ray free electron lasers [2] and advanced accelerators [3] require electron beams of ultra-high brightness. The power of SR grows nonlinearly with the beam brightness or energy, and therefore nonlinear beam dynamics inevitably arises due to the strong near-field SR. For instance, the coherent SR fields may cause collective beam instabilities such as longitudinal energy modulation, and increase the beam emittance; the incoherent fields may generate random shot noises and phase space diffusion, leading to beam quality degradation.

Different from the far-field SR, it remains a challenge to directly characterize the near-field SR in experiments. Several simulation models have therefore been considered [4]. Standard beam design tools mostly treat the Liénard-Wiechert (LW) potential and adopt the steady-state assumption. This approach is generally not self-consistent by ignoring the temporal dependence of the emission, and hence is only suitable for describing the linear stage of the instability growth. On the other hand, the particle-mesh models via discretization

of the full-wave Maxwell equations (e.g. Finite Difference Time Domain, FDTD) are self-consistent for the coherent effects, but their accuracy is severely limited by numerical errors due to numerical dispersion and numerical Cherenkov instability.

In this study, we investigate a novel near-field method that can potentially overcome the above issues. In this original idea proposed by Shintake [5], one calculates radiation fields at the current position and then propagates them outwards to obtain real-time fields at nearby locations. By mapping the fields onto a co-moving mesh, it allows for greatly reduced propagation errors in comparison to the FDTD method. Most importantly, it allows for real-time selection of the temporal information that is only relevant to the current beam-radiation interaction. This can be much more efficient than the LW method where complete emission history has to be kept for reconstructing fields at the present time.

So far, the Shintake's near-field (SNF) method has been mainly used to construct field patterns in nearby zones. The calculation of the fields remains to be verified. As a first step towards building a comprehensive framework, we provide a validation of the field calculation by applying it to a fixed observation point near the electron trajectory. We discovered that the original idea of Shintake missed the important term of the acceleration field and applied only to linear electron motion. To correct this limitation we come up with complete steps that can accurately determine the fields at arbitrary positions. As we shall see, the modified algorithm gives consistent field calculations with the LW equation. Some basic signatures of the near-field SR due to cyclotron motion are also explored with the updated method.

## SHINTAKE'S NEAR-FIELD METHOD

In the original idea [5], a moving electron emits wavelets of electromagnetic fields which form a set of outgoing spherical waves in free space by following the wave equation. Once emitted, the spherical wavefronts will expand outwards at the speed of light. The centers of these spheres emitted at different times, however, shift in positions due to the electron motion. The wavelet propagation direction is related to the electron instantaneous velocity at the time of emission, and is given by the Lorentz transformation of the unit propagation vector  $\vec{k}$  (essentially a displacement vector) from the electron to the lab frame:  $k_x = (\cos \theta' + \beta)/(1 + \beta \cos \theta')$ ,  $k_y = \sin \theta'/\gamma(1 + \beta \cos \theta')$ , where  $\theta'$  is the propagation angle in the electron frame relative to the electron velocity  $\vec{\beta}$  (normalized by  $c$ ), and  $\gamma = 1/\sqrt{1 - \beta^2}$  is the electron's Lorentz factor.

\* Work supported by the LDRD program at LANL.

<sup>†</sup> fyli@lanl.gov

Content from this work may be used under the terms of the CC BY 3.0 licence (© 2019). Any distribution of this work must maintain attribution to the author(s), title of the work, publisher, and DOI

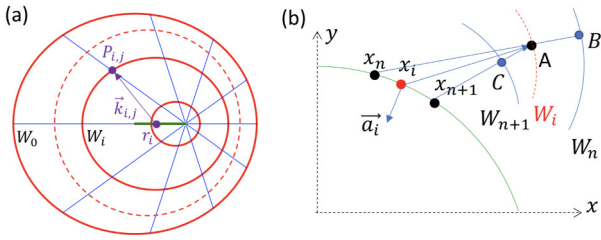


Figure 1: (Color online). (a) Wavelet trajectories (blue lines) and wavefronts (red lines) for an electron of  $\gamma = 1.1$  performing a linear motion (green line); (b) Schematic of a trajectory interpolation to find the intermediate position  $x_i$  from which the emitted wavefront  $W_i$  exactly crosses the fixed point  $A$  at time  $t$ .

With the  $\vec{k}$  vectors found, one can obtain the positions of the wavelets on the  $i$ -th wavefront,  $W_i$ , at the  $N$ -th time step ( $N > i$ ) by

$$\vec{P}_{i,j}(N\Delta t) = \vec{r}_i + c(N-i)\Delta t \vec{k}_{i,j}, \quad (1)$$

where  $j$  is the index of the wavelet directions, and  $\vec{r}_i = \vec{r}_0 + \sum \vec{v}(m\Delta t)\Delta t$  (where the sum is over  $m = 1, 2, \dots, i$ ) is the electron position at the time of emitting the  $i$ -th wavefront. Figure 1(a) shows the resulting field pattern due to a linear electron motion. Notice that, by Eq. (1) one actually tags the outermost wavefront as  $W_0$ , therefore avoids iterating all the wavefronts at each time step as opposed to the original proposal [5] where the innermost is tagged as  $W_0$ .

## VALIDATION OF FIELD CALCULATION

In SNF method, fields are defined on the wavefronts. To obtain fields in a position not on the wavefronts, one may interpolate the fields at adjacent wavelets to the fixed point, but it can introduce errors especially when vastly different spatial scales (due to incoherent and coherent SR fields) are involved. Instead, we consider finding the retarded electron position from which the emitted wavefront exactly crosses the point at the observation time. This is essentially an interpolation of the electron trajectory, and the fields obtained in this manner are precise except for the approximations made in discretizing the electron motion.

### Trajectory Interpolation

Figure 1(b) shows a sketch for the trajectory interpolation.  $A$  is the fixed point.  $W_n$  and  $W_{n+1}$  are the most adjacent wavefronts that were emitted at the space-time  $(x_n, t_n)$  and  $(x_{n+1}, t_{n+1})$ , respectively. To find the exact point  $x_i$  (so the exact wavefront  $W_i$ ), we first locate the segment  $[x_n, x_{n+1}]$  within which  $x_i$  resides; this can be achieved by using the geometric relations:

$$|x_n \vec{B}| \geq |x_n \vec{A}|; |x_{n+1} \vec{A}| > |x_{n+1} \vec{C}|, \quad (2)$$

where  $|x_n \vec{B}| = c(t - t_n)$  and  $|x_{n+1} \vec{C}| = c(t - t_{n+1})$ .

Then the exact point  $\vec{x}_i = \vec{x}_n + \vec{v}_n(t_i - t_n)$  can be obtained by solving  $t_i$  from the quadratic equation:

$$c(t - t_i) = |x_i \vec{A}| = |\vec{x}_A - [\vec{x}_n + \vec{v}_n(t_i - t_n)]|, \quad (3)$$

where  $\vec{v}_n = \vec{v}(\vec{x}_n)$ . Notice that, in the above equation the electron velocity during  $[x_n, x_{n+1}]$  is fixed due to the discretization of electron trajectory.

### Double Lorentz Transformation

The vector pointing from the emitter to the observer is  $\vec{r} = \vec{x}_A - \vec{x}_i$ . In order to calculate the fields at the fixed point, it is conceptually simplest to perform double Lorentz transformation to and from the electron instantaneous rest frame along axes projected by the electron velocity  $\vec{\beta}_i = \vec{\beta}_n$ . Below we use the subscript 1 to represent the longitudinal component along  $\vec{\beta}_n$  and 2 the transverse component. The  $\vec{r}$  vector is transformed to the electron frame by  $r'_1 = \gamma(r_1 - \beta\Delta t)$ ,  $r'_2 = r_2$ , where  $\Delta t = |\vec{r}|/c = t - t_i$  is the time difference between the observer time and the retarded time in the lab frame. In the electron frame, we first consider the fields due to the charge at rest, which is given on the corresponding wavefront by

$$\vec{E}'_{\text{vel}} = -e\hat{n}'/r'^2, \quad (4)$$

where  $\hat{n}' = \vec{r}'/r'$ . Transforming back to the lab frame, we have  $E_1 = E'_1$ ,  $E_2 = \gamma E'_1$ . The field is also partially converted into magnetic field as  $B_3 = \gamma\beta E'_2$ .

In the original SNF method, only the above velocity field is considered which only applies to a linear motion. However, for a nonlinear motion, non-inertial force or acceleration is also present in the instantaneous rest frame. For the fields due to the acceleration only, one can calculate according to

$$\vec{E}'_{\text{accel}} = e \frac{\hat{n}' \times (\hat{n}' \times \vec{a}')}{r'}, \quad (5)$$

where  $\vec{a}' = d\vec{\beta}'/dt'$  is the acceleration in the electron frame. For a cyclotron motion, there is only transverse acceleration  $\vec{a}'_{\perp}$  which transforms as  $\vec{a}'_{\perp} = \gamma^2 \vec{a}_{\perp}$ . When transforming the acceleration field back to the lab frame, there are also magnetic field  $B'_{\text{accel}} = \hat{n}' \times \vec{E}'_{\text{accel}}$  added to the transverse component through  $E_2 = \gamma(E'_1 + \beta B'_{\text{accel}})$ .

### Benchmarks and Basic Radiation Signatures

To validate the above scenario, we apply it to a cyclotron motion of radius  $R = 1$  m,  $\gamma = 200$  and a fixed point off the reference trajectory by  $R_{\text{off}} = 1 \times 10^{-4}R$ . All the other quantities are normalized properly to  $R$ , e.g.,  $t$  to  $R/c$ , length to  $R$ , and cyclotron frequency  $\omega_c$  to  $c/R$ . The results are shown in Fig. 2 and compared to the LW equation (primes indicate quantities at the retarded time),

$$\vec{E}' = \frac{e(\hat{n}' - \vec{\beta}')}{\gamma^2 r'^2 (1 - \hat{n}' \cdot \vec{\beta}')} + \frac{e\hat{n}' \times [(\hat{n}' - \vec{\beta}') \times \vec{\beta}']}{r'(1 - \hat{n}' \cdot \vec{\beta}')}. \quad (6)$$

For the latter, the fields are directly calculated at the electron time,  $t_e$ , and the observation time is corrected by the

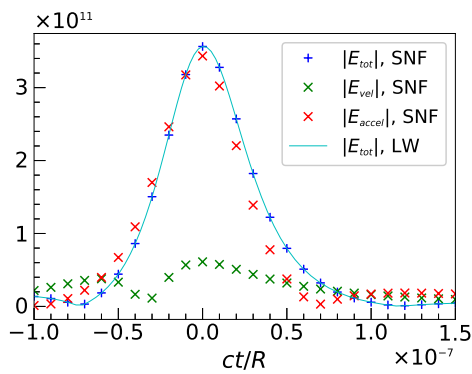


Figure 2: Comparison of the SNF calculation with the LW equation for a fixed point near the trajectory of a cyclotron motion.

time needed to propagate the fields from the emitter to the observer,  $t = t_e + r(t_e)/c$ ; this suggests the observation time for this direct approach is non-uniform. Good agreement is achieved in the total field amplitude, and the fields are dominated in this case by the acceleration field.

Finally, with the above scenario we also study some basic signatures of the near-field SR due to a cyclotron motion. Figures 3(a) and (b) show the dependences of the velocity field and acceleration field with the electron energy  $\gamma$ ; the temporal behavior of both scales exactly as  $\gamma^3$ , but for the amplitude the acceleration field scales as  $\gamma^{3.5}$  and the velocity field scales as  $\gamma^2$  (minor difference appears for the field maximum). Notice that, these trends are valid for the near field at a distance scaled with  $\gamma$  as  $R_{\text{off}} = 10^{-4}R\gamma$ . This self-similarity of the fields is an important signature of the near-field SR [6]. The dependence of the total fields with  $R_{\text{off}}$  shown in Fig. 3(c) is less trivial: it roughly changes as  $R_{\text{off}}^{-0.5}$  in the near field, i.e.,  $R_{\text{off}} \ll 1$ , but deviates greatly from the trend in the far field as soon as  $R_{\text{off}} \geq 1$ . However the temporal behavior is basically invariant for different distances. The latter is confirmed in the spectra (for the  $x$  component of the total field) presented in Fig. 3(d) which shows similar critical frequency despite of lower amplitudes for larger  $R_{\text{off}}$ . A difference in the far-field spectra from the near-field ones is the loss of the low-frequency (or long-wavelength) components; this is due to the fact that the velocity field, essentially long-wavelength space-charge field, is limited to the near field. The critical photon energy is consistent with the formula  $E_c(\text{keV}) = 0.665E_e^2(\text{GeV})B(\text{T})$ , where  $E_e$  is the electron energy and  $B$  is the applied bending magnetic field.

## SUMMARY

In summary, we have examined the field calculation of Shintake's method for modeling near-field SR. It is discovered that the original idea of Shintake missed the important acceleration fields which are prevalent for a nonlinear motion. To correct this limitation a modified scenario combining a trajectory interpolation and a double Lorentz transformation is implemented, which gives consistent field calculations

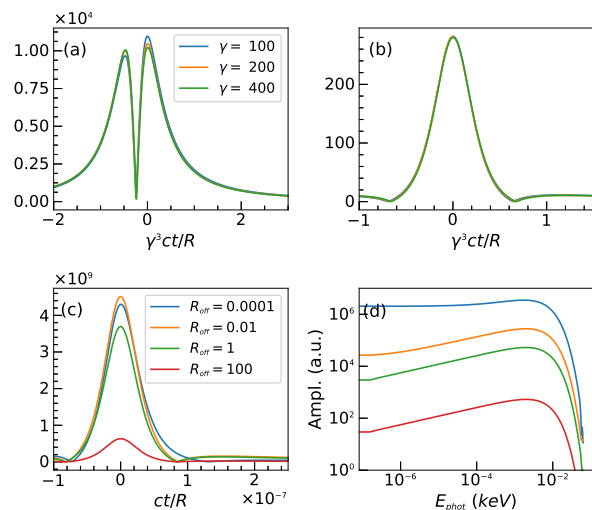


Figure 3: (a) The velocity field (scaled down by  $\gamma^2$ ) and (b) the acceleration field (scaled down by  $\gamma^{3.5}$ ) for different  $\gamma$ , where  $R_{\text{off}}$  is scaled with  $\gamma$  as  $10^{-4}R\gamma$ ; (c) The total fields (scaled up by  $R_{\text{off}}^{0.5}$ ) for different  $R_{\text{off}}$  and (d) corresponding spectra for the  $x$  component of the total fields, where  $\gamma$  is fixed to be 200.

with the Liénard-Wiechert equation. Some basic signatures of the near-field SR have also been obtained by applying this modified approach to a cyclotron motion.

## ACKNOWLEDGEMENTS

Research presented in this article was supported by the Laboratory Directed Research and Development Program of Los Alamos National Laboratory (LANL) under the project number 20190131ER. Computations were supported by the Institution Computing Program at LANL.

## REFERENCES

- [1] M. Chergui and A. H. Zewail, "Electron and x-ray methods of ultrafast structural dynamics: Advances and applications", *ChemPhysChem*, vol. 10, no. 1, pp. 28–43, 2009.
- [2] B. W. McNeil and N. R. Thompson, "X-ray free-electron lasers", *Nature photonics*, vol. 4, no. 12, p. 814, 2010.
- [3] E. Esarey, C. Schroeder, and W. Leemans, "Physics of laser-driven plasma-based electron accelerators", *Reviews of modern physics*, vol. 81, no. 3, p. 1229, 2009.
- [4] G. Bassi *et al.*, "Overview of csr codes", *Nuclear Instruments and Methods in Physics Research Section A: Accelerators, Spectrometers, Detectors and Associated Equipment*, vol. 557, no. 1, pp. 189–204, 2006.
- [5] T. Shintake, "Real-time animation of synchrotron radiation", *Nuclear Instruments and Methods in Physics Research Section A: Accelerators, Spectrometers, Detectors and Associated Equipment*, vol. 507, no. 1-2, pp. 89–92, 2003.
- [6] C. Huang, T. J. Kwan, and B. E. Carlsten, "Two dimensional model for coherent synchrotron radiation", *Physical Review Special Topics-Accelerators and Beams*, vol. 16, no. 1, p. 010701, 2013.